

Cloaking waveguide defects at low frequencies using local wall deformations

Author Names(s): Daria Zyla-Jablonska, Tomasz Bobinski

Division of Aerodynamics, Faculty of Power and Aeronautical Engineering,
Warsaw University of Technology, Poland
daria.zyla.dokt@pw.edu.pl

1 INTRODUCTION

From the perspective of coastal engineering, efficient control of the propagation of surface water waves is of great importance. Various methods can be employed to achieve controlled propagation of surface water waves. One such approach is using metamaterials – materials with a specific, periodic structure at the subwavelength scale, which enable the realization of phenomena unattainable with conventional materials found in nature [1]. One of the most exciting applications of metamaterials is the cloaking phenomenon, in which an object becomes invisible. In the context of surface water waves, cloaking can be achieved using different approaches. The first involves designing the bathymetry around the object to be hidden [2]. Other options include surrounding the object with an array of structured elements piercing the free surface [3], or altering the boundary conditions at the free surface by surrounding the object with a floating elastic composite plate [4].

In this work, we propose a novel technique for designing a cloak. We focus on cloaking a defect in the form of a surface-piercing vertical cylinder placed symmetrically within a water waveguide system in the low-frequency range. We show that by locally varying the shape of the waveguide walls, we can significantly reduce the backscattering produced by the cylinder. We use an optimization process to design the shape of the wall in the vicinity of the cylindrical defect, and we quantitatively confirm its broadband character through experiments.

2 MODELING

2.1 Governing equations

The reference model in our analysis is a system with harmonic linear surface water waves propagating within a parallel waveguide of width L characterized by a flat bottom and a surface-piercing cylinder of diameter $D = 0.6L$ positioned at the plane of symmetry. In the analyzed case, wave propagation is described by the two-dimensional Helmholtz equation

$$\Delta\eta(x, y) + k^2\eta(x, y) = 0 \tag{1}$$

with Neumann boundary conditions $\nabla\eta \cdot \vec{n} = 0$ at the waveguide's rigid walls ($y = \pm L/2$) and the cylinder ($x^2 + y^2 = D^2/4$) with $\eta = \eta(x, y)$ being free surface deformation, k being a wavenumber following the linear dispersion relation $\omega^2 = gk \tanh(kh)$ where g represents the gravity constant, ω denotes frequency and h is water depth. We consider the low frequency range $kL/\pi < 1$, in which only plane wave propagates. The solution can be expressed as $\eta(x) = Ae^{ikx} + AR e^{-ikx}$ in the far-field ahead of the cylinder, and $\eta(x) = AT e^{ikx}$ in the far-field behind the cylinder (A denotes the amplitude of the incident wave, R and T denote the reflection and transmission coefficients, respectively).

2.2 Cloak design

Reflection is absent for an ideal broadband cloak ($R = 0$), ensuring perfect transmission ($T = 1$) over a wide range of frequencies. In this work, we aim to make the cylinder invisible to incident waves over a broad range of frequencies by creating narrow indentations in the waveguide walls near the obstacle, which are symmetrical with respect to the cylinder. We minimize the cloaking factors χ and χ_{sc} based on reflected and total scattered energy to determine the specific shape of the walls' indentations

$$\chi = \frac{\int_{k_1}^{k_2} |R|^2 dk}{\int_{k_1}^{k_2} |R_0|^2 dk} \quad (2) \quad \chi_{sc} = \frac{\int_{k_1}^{k_2} (|R|^2 + |T - 1|^2) dk}{\int_{k_1}^{k_2} (|R_0|^2 + |T_0 - 1|^2) dk} \quad (3)$$

where R_0, T_0 denotes the reflection and transmission coefficient for the reference case with straight parallel walls, respectively. We solve the problem using the finite element method implemented in the MATLAB PDE Toolbox. We assume a Sommerfeld condition at the outlet $\partial_x \eta = ik\eta$, a Dirichlet condition at the inlet $\eta = 1$, and a Neumann condition on the rigid walls $\nabla \eta \cdot \vec{n} = 0$.

The shape of the walls near the obstacle is generated using a cosine Fourier series with parameters defining geometry, such as the length of the region with variable geometry, depth, number of grooves, and the shape of individual grooves. The cloak geometry is obtained within an optimization process employing the Surrogate Optimization solver. The optimization process involves mesh generation, solving the Helmholtz equation, and calculating the cloaking factor.

2.3 Numerical results

For surface water waves, a cloaking device modifies the scattered field and the forces acting on an object. In the considered problem, the force acting on a fixed body can be determined by integrating the pressure over the body surface, which can be expressed as[5]

$$\overline{\vec{F}^{(2)}} = \frac{1}{T} \int_0^T \left(-\frac{1}{2} \rho g \int_{z=0} (\eta^{(1)})^2 \cdot \vec{n}_s d\ell + \frac{1}{2} \rho \int_S (\nabla \Phi^{(1)})^2 \cdot \vec{n}_s dS \right) dt \quad (4)$$

Here, S , \vec{n}_s , and $d\ell$ denote the wetted body surface, the unit normal vector, and an infinitesimal segment along the water contour at $z = 0$, respectively. $\eta^{(1)}(x, y, t) = \text{Re}(\eta \cdot e^{-i\omega t})$ and $\Phi^{(1)}(x, y, z, t) = \text{Re}(\Phi \cdot e^{-i\omega t})$ represent the first-order surface elevation and velocity potential, respectively.

Minimizing the cloaking factor χ results in a geometry depicted in Fig.1a by the solid blue line (denoted as Fourier) with $\chi = 5.44 \cdot 10^{-5}$. The optimized (Fourier) shape closely resembles a trapezoid; hence, we introduced a simplified geometric approximation and performed a subsequent optimization. Figure 1b compares the reflection coefficient between the reference case (uncloaked) and the following optimized cloaked cases: Fourier, trapezium, and rectangular geometries. The shape simplification had a negligible impact on the numerical results while significantly streamlining the fabrication process for the experimental implementation. Figure 1c shows a comparison of the mean horizontal drift forces between the reference and cloaked cases, respectively. Implementing a cloaking device significantly reduces backscattering and substantially decreases the horizontal force acting on the surface-

piercing cylinder across the entire considered frequency range, with the maximum force below 2% of the reference case.

We perform a similar analysis for the cloaking factor χ_{sc} that considers the phase shift. However, minimizing χ_{sc} results in significantly higher backscattered energy, leading us to focus on the geometry optimized for χ in our experiments.

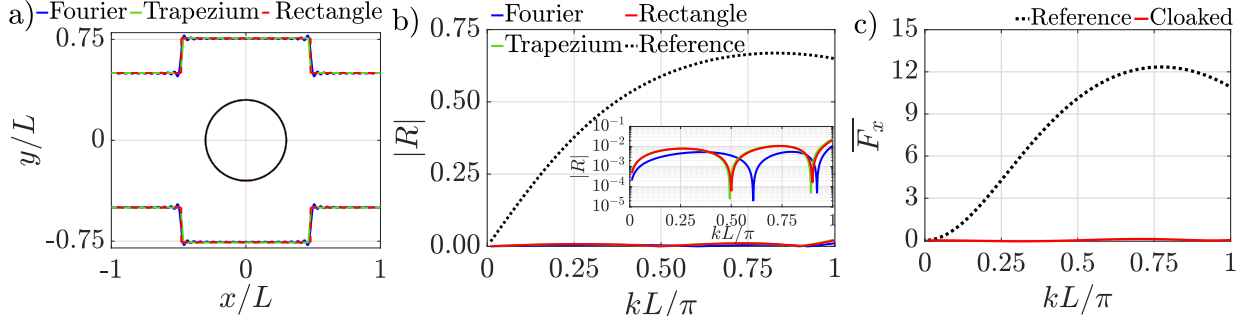
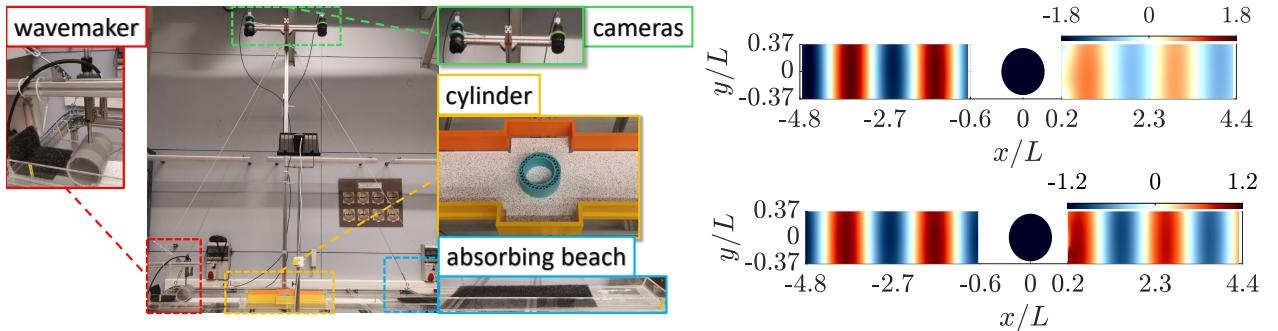


Figure 1: (a) Geometries providing cloaking phenomenon: Fourier, trapezium and rectangular geometry. (b) The reflection coefficients. (c) The mean horizontal forces.

3 EXPERIMENTAL REALIZATION

Experimental arrangements

Figure 2a illustrates the measurement setup consisting of a straight channel with vertical walls, a digitally controlled LinMot wavemaker, a cylindrical obstacle, an absorbing beach, a light source, and two BASLER cameras. The still water level is $h = 2 \pm 0.05$ cm, the waveguide width $L = 16$ cm, and the obstacle diameter $D = 9.6$ cm. We examine two waveguide geometries: one with straight parallel walls (reference case) and another with a cylinder cloak in the form of rectangular cavities. We generate waves in the frequency range from 0.65Hz to 1.36Hz, corresponding to $kL/\pi \in (0.53, 0.97)$. We perform measurements of



(a) Experimental setup.

(b) $\text{Re}(\eta)$ of the extracted wave fields for $f = 1.32$ Hz ($kL/\pi \approx 0.94$).

Figure 2: Experimental realization

the elevation of the free surface using a combination of the Optical Flow (OF) [6] technique and the synthetic Schlieren (SS) technique ([7]).

Results and analysis

Using free surface deformation fields, we perform the Fourier transform in time. We isolate the plane mode based on these wave fields and determine the coefficients of reflection R and transmission T . Figure 2b presents examples of the real parts of η normalized by the wave

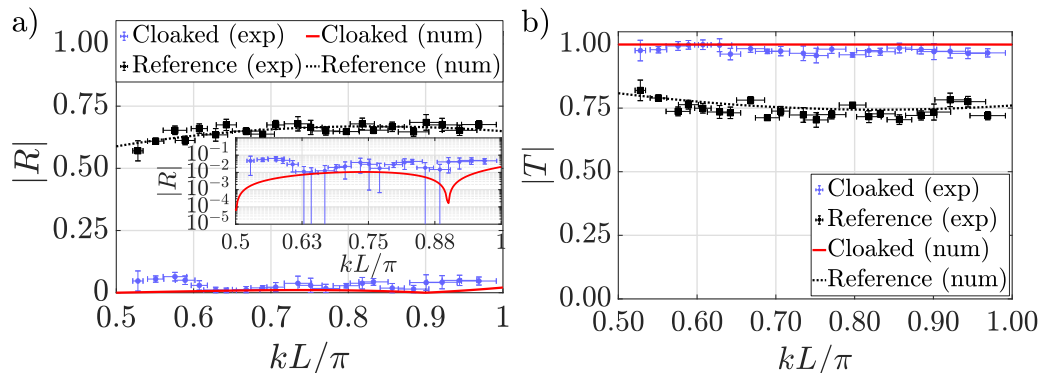


Figure 3: (a) Reflection coefficient (b) Transmission coefficient

amplitude. The upper image corresponds to the uncloaked case, showing strong reflections in front of the cylinder, while the lower image represents the cloaked case for $kL/\pi \approx 0.94$. In Figure 3 we present a comparison of both coefficients as a function of kL/π obtained in numerical simulations and experiments. Figures 3a and 3b illustrate a significant reduction in the reflection coefficient and a substantial increase in transmission, respectively, both observed throughout the frequency range. It can be observed that the reflection coefficient decreases by at least an order of magnitude compared to the straight parallel waveguide. However, the experimental results are not as favourable as the numerical predictions.

CONCLUSIONS

This work presents a novel technique for achieving an invisibility effect in a water wave system with a circular cylinder placed symmetrically within a parallel waveguide. We obtain the broadband cloaking phenomenon by considering local waveguide wall deformations near the cylinder. We confirm the high efficiency of the proposed technique experimentally, where the energy of the reflected wave is at least 100 times lower than in the reference case in the entire frequency range.

REFERENCES

- [1] Zhu, Zhao, Han et al. (2024) Controlling water waves with artificial structures. *Nat Rev Phys* 6, 231-245
- [2] Porter, R. Newman, J. N. (2014) Cloaking of a vertical cylinder in waves using variable bathymetry. *Journal of Fluid Mechanics* 750, 124–143.
- [3] Newman, J.N. (2014) Cloaking a circular cylinder in water waves. *European Journal of Mechanics - B/Fluids* 47, 145–150.
- [4] Iida, Takahito, Zareei, Ahma, Alam, Mohammad-Reza (2023) Water wave cloaking using a floating composite plate. *Journal of Fluid Mechanics* 954, A4.
- [5] Dupont G, Guenneau S, Kimmoun O, Molin B, Enoch S. (2016) Cloaking a vertical cylinder via homogenization in the mild-slope equation. *Journal of Fluid Mechanics* 796:R1
- [6] Farneback, G. (2003). Two-Frame Motion Estimation Based on Polynomial Expansion. Bigun, J., Gustavsson, T. (eds) *Image Analysis*. SCIA 2003. Lecture Notes in Computer Science, vol 2749.
- [7] Moisy, F., Rabaud, M., Salsac, K. (2009). A synthetic Schlieren method for the measurement of the topography of a liquid interface. *Experiments in Fluids* 46. 1021-1036.